International Journal of Biochemistry and Cell Biology 112 (2019) 24–38

Contents lists available at ScienceDirect

International Journal of Biochemistry and Cell Biology

journal homepage: www.elsevier.com/locate/biocel

Psammaplysin F increases the efficacy of bortezomib and sorafenib through regulation of stress granule formation

Kimberley E. Christen[a,b], Rohan A. Davis[a,b], Derek Kennedy[a,b,*]

[a] Griffith Institute for Drug Discovery, Griffith University, Brisbane, QLD, 4111, Australia
[b] School of Environment and Science, Griffith University, Brisbane, QLD, 4111, Australia

ARTICLE INFO

Keywords:
Stress granules
Psammaplysin F
Natural product
eIF2α
Bortezomib
Sorafenib

ABSTRACT

The past few decades have delivered significant improvements in diagnosis and treatment of cancer, however, despite these improvements cancer continues to be a major global health issue requiring the urgent development of new strategies for treatment. Stress granules are cytoplasmic structures that triage gene expression in response to environmental stresses, including chemotherapies, and have been implicated in the development of drug resistance. One novel approach to developing a new anti-cancer strategy involves inhibiting stress granules with compounds derived from natural products. In a previous rapid screen, a subset of 132 compounds from the Davis Open Access Natural Product Library was screened using a stress granule inhibition assay and provisionally one hit was identified which was the known marine sponge-derived metabolite, psammaplysin F. Using cell based assays psammaplysin F was assessed to determine whether it could inhibit the formation of stress granules after exposure to sodium arsenite in Vero, HEK293 MCF7, T47D, HeLa and MCF7MDR cells by analysing the number of stress granules using high content imaging. A significant reduction in the number of stress granules was observed and subsequent analysis by western blot revealed that treatment with psammaplysin F decreased levels of phosphorylated eIF2α. Combinational studies in MCF7, HeLa and MCF7MDR cells revealed that psammaplysin F increased the efficacy of bortezomib and sorafenib and a synergistic effect was observed *in vitro*. Stress granules appear to be one tool in a battery of responses that cancer cells can exploit to elicit drug resistance. Disrupting stress granule formation by use of orally available drugs presents a potential mechanism to restore drug efficacy. The work presented here provides evidence that small molecules derived from nature, such as psammaplysin F, can prevent the formation of stress granules and therefore may represent a useful strategy to improving drug efficacy.

1. Introduction

Cancer is one of the leading causes of death worldwide and despite significant improvements to treatment and prevention, the number of new cases continues to increase (Global Burden of Disease Cancer, 2017; Wang et al., 2016). Systemic therapies are used to treat patients with cancer, however, chemotherapeutics often lack specificity and not only kill cancer cells but also normal, healthy cells in the patient. Furthermore, cancer cells have the capacity to become resistant to chemotherapeutic treatment (Housman et al., 2014). Therefore, new treatments need to be developed to overcome this problem and a novel approach to combat the effect of resistance is the disruption of stress granules (SGs).

SGs are ribonucleoprotein particles (RNP) that are formed in the cytoplasm of eukaryotic cells (Kedersha et al., 2000) in response to stresses such as heat, oxidative conditions, UV irradiation, hypoxia, hydrogen peroxide, viral infection and chemotherapeutics (Emara et al., 2012, Fournier 2010; Kaehler et al., 2014; Kedersha and Anderson, 2007; Takahashi et al., 2013). During cellular stress, transcripts encoding housekeeping proteins are redirected from polysomes to SGs (Kedersha et al., 2005, Matsuki 2013) and cells redirect the specific expression of proteins, such as heat shock and cytoprotective proteins, required to survive the environmental stress.

In many cells SGs cannot form without RNA-binding proteins such as T-cell intracellular antigen 1 (TIA1) and Ras-GTPase activating protein-binding protein 1 (G3BP1) which contain aggregation-prone

Abbreviations: G3BP1, ras-GTPase activating protein SH3-domain-binding protein 1; HRI, heme regulated eukaryotic initiation factor 2 alpha kinase; eIF2α, eukaryotic initiation factor 2 alpha; p-eIF2α, phosphorylated eukaryotic initiation factor 2 alpha; RNP, ribonucleoprotein particles; SA, sodium arsenite; SGs, stress granules

* Corresponding author at: Griffith Institute for Drug Discovery, Griffith University, Brisbane, QLD, 4111, Australia.
E-mail address: derek.kennedy@griffith.edu.au (D. Kennedy).

https://doi.org/10.1016/j.biocel.2019.04.008
Received 1 November 2018; Received in revised form 24 March 2019; Accepted 19 April 2019
Available online 22 April 2019
1357-2725/

domains to mediate SG assembly (Anderson et al., 2014, Hofmann 2012). Many of the SG-associated RNA-binding proteins are capable of shuttling between the nucleus and the cytoplasm, presumably to translationally active sites. The relocation and aggregation of RNA-binding proteins, and their mRNA cargo, within the cytoplasm in response to environmental stress and activation of specific signalling pathways is considered one mechanism by which SG formation is initiated (Bounedjah et al., 2014). The cellular mechanisms that drive RNA-binding proteins and their cargo to form SG is not completely characterised, however, one common theme appears to be blockage of translational initiation. The most commonly characterised way to do this is by phosphorylation of eIF2α (Anderson et al., 2015). The phosphorylation of eIF2α reduces the availability of the ternary complex, eIF2-GTP-$tRNA_i^{Met}$ (Gilks et al., 2004; Kedersha and Anderson, 2007; Kedersha et al., 2000; McInerney et al., 2005). This ternary complex loads the initiator tRNA onto the 40S ribosomal subunit in a GTP-dependent manner and interacts with other core translation initiation factors to form the 48S pre-initiation complex (Gilks et al., 2004). The 48S complex binds to the start codon and the 60S ribosomal subunit is recruited to form an 80S ribosome. Therefore, the phosphorylation of eIF2α results in the inhibition of translation initiation by reducing the availability of the ternary complex and subsequently resulting in the formation of SGs (Anderson et al., 2014, Gilks 2004).

There are four kinases in mammalian cells that phosphorylate eIF2α; the endoplasmic reticulum-localised eIF2α kinase which recognises ER stress, the mammalian homologue of yeast which recognises nutrient availability, the double-stranded RNA activated protein kinase which recognises double-stranded RNA and the heme-regulated eukaryotic initiation factor 2 alpha kinase (HRI) which recognises oxidative stress and heme deficiency (Anderson and Kedersha, 2009; McEwen et al., 2005; Reineke et al., 2012). These kinases share extensive homology in their kinase catalytic domain and they all phosphorylate eIF2α on serine 51 (Lu et al., 2001). Sodium arsenite (SA) is a pharmacological activator of HRI, and induces the phosphorylation of eIF2α and subsequently the formation of SGs (Ghisolfi et al., 2012) by oxidative stress and the formation of reactive oxygen species (Ruiz-Ramos et al., 2009), therefore representing a useful tool for the induction of SGs in *in vitro* models.

There is significant protein heterogeneity in SGs and this would appear to match the dynamic range of mRNA cargo they carry (Buchan and Parker, 2009; Smith et al., 2014). To date a specific consensus of transcripts triaged by SGs has not been defined, however, another theme that has immerged from ongoing studies suggests that translational silencing of mRNA *via* SGs appears to be bias towards housekeeping genes (Anderson and Kedersha, 2006). Furthermore, sub-populations of transcripts appear to be specifically excluded from silencing in SGs and one interesting example includes drug resistance genes. The expression of at least one drug resistance protein, P-glycoprotein (also known as multidrug resistance 1 or MDR1), appears to be regulated at the level of translation, however, its transcripts are not sequestered to SGs (Yagüe and Raguz, 2010). This data leads to the exciting possibility that disrupting SG formation during chemotherapy may change the balance of translation within cells and abrogate some drug resistance and restore efficacy of a specific drug. In 2010 Fournier *et al.* (Fournier et al., 2010), demonstrated that this was possible. In their studies they demonstrated that bortezomib treatment in HeLa cells caused the formation of SGs and showed that this correlated to a loss of drug efficacy. However, when they knocked-down expression of HRI, which is responsible for eIF2α phosphorylation under osmotic, heat and oxidative stresses, they demonstrated that cytotoxic activity of bortezomib could be, at least partially, restored (Fournier et al., 2010). The knock-down of HRI and restoration of drug cytotoxicity provides a proof of concept that regulating SG formation may be a strategy that can be used in conjunction with systemic therapies to maintain or even augment drug potency. However, technologies cannot yet deliver tissue-specific knock-down of genes in animal systems. Therefore, another solution needs to be found and this could potentially involve the of compounds that disrupt SG formation.

Natural products have been used for decades in the treatment of cancer (Demain and Vaishnav, 2011) with 60% of current anti-cancer drugs derived from natural sources (Cragg and Newman, 2009). Natural products are derived from biota (*e.g.* plants, marine invertebrates, microbes, etc) found in terrestrial and marine environments (Demain and Vaishnav, 2011) and are typically small secondary metabolites with structural diversity that contribute to the organisms survival (Basmadjian et al., 2014). These unique compounds have been optimised by nature over the millennia and have evolved to bind to biological targets, such as proteins/enzymes and receptors (Basmadjian et al., 2014). We hypothesised that natural products could hold the key to discovering potentially druggable compounds that could inhibit SG formation. Therefore, a pure compound natural product library was chosen for screening in our SG-based cancer program as the novel structural diversity of such a library was predicted to increase the chances of identifying a compound that inhibits SG formation.

Psammaplysin F was first isolated in 1997 from a marine sponge that belonged to the genus *Aplysinella* (Liu et al., 1997). Psammaplysin F has reported activity against the malaria parasite displaying some selectivity against chloroquine-resistant and chloroquine-sensitive *Plasmodium falciparum* lines (IC_{50} 1.38 μM and 0.867 μM, respectively) when compared to HEK293 cells (IC_{50} of 10.9 μM) (Xu et al., 2010). This marine natural product also demonstrated activity against Gram-positive bacteria by inhibiting cell division and preventing the partitioning of chromosomes (Ramsey et al., 2013). Recently, psammaplysin F has shown moderate growth inhibition against *Trypanosoma cruzi* with an IC_{50} of 5.63 μM (Zulfiqar et al., 2017).

There have been no reported cases to date of natural products inhibiting SG formation. We report for the first time, a natural product that can disrupt the formation of SGs by inhibiting the phosphorylation of eIF2α.

2. Materials and methods

2.1. Human cell cultures

HEK293, MCF7, T47D, HeLa and Vero cells (purchased from ATCC) were maintained in DMEM/F12 media with L-glutamine and sodium bicarbonate (Corning) and supplemented with 10% fetal bovine serum (FBS) (Life Technologies) in an incubator at 37 °C and 5% CO_2. Medium was changed every 2 days until the cells reached 80% confluence. Cells were grown up to 30 passages and then discarded.

2.2. Development of the MCF7MDR cell line

MCF7 cells were maintained in DMEM/F12 media with L-glutamine and sodium bicarbonate (Corning) and supplemented with 10% fetal bovine serum (FBS) (Life Technologies) in an incubator at 37 °C and 5% CO_2. The MCF7MDR cell line was derived from the parental MCF7 cells following long term (> 12 months) culture in a medium supplemented with cisplatin (CDDP) and fluorouracil (5-FU). A resistance index (RI) was determined for the MCF7MDR cells to determine the drug resistance of the cell line. The RI was calculated as the ratio of the IC_{50} of the MDR cell line/IC_{50} of non-treated MCF7 cell line. The RI of MCF7MDR cells against 5-FU was 2.7, while CDDP was 1.3.

2.3. In vitro stress granule assay

HEK293, MCF7, T47D, Vero, HeLa and MCF7MDR cells were trypsinised (Life Technologies) once 80% confluence was reached and pelleted in a centrifuge for 5 min. at 0.3 rcf. Cells were resuspended in 1 mL of media and seeded onto coverslips for later microscopy. HEK293, Vero and HeLa cells were seeded onto coverslips in 24-well plates at a density of 100,000 cells per well. MCF7, T47D and

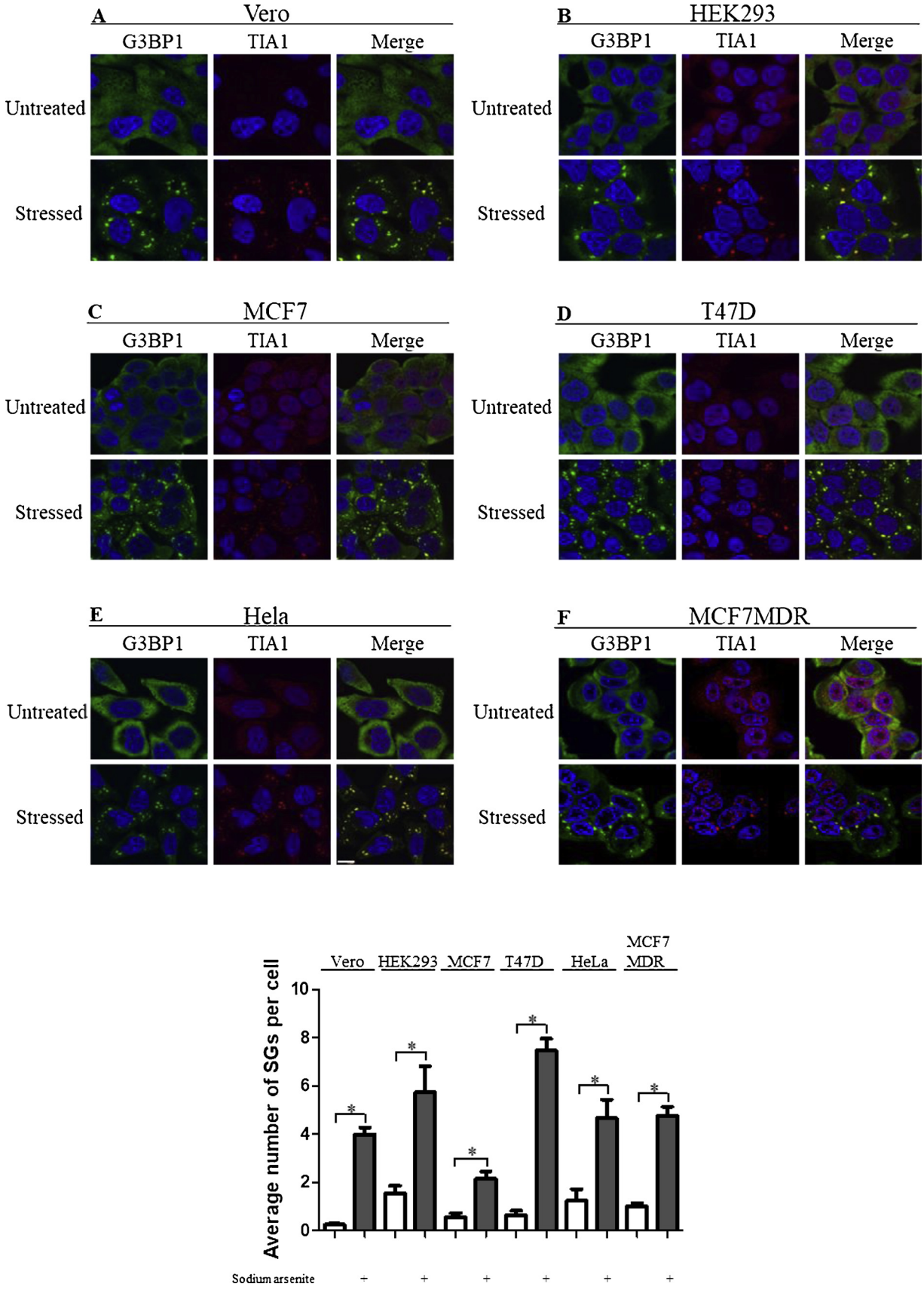

Fig. 1. Sodium arsenite causes stress granule formation. (A) Vero cells treated with sodium arsenite at 500 μM for 1 h to form SGs (stressed, lower row) *versus* untreated cells (upper row). **(B)** HEK293, **(C)** MCF7 and **(D)** T47D cells treated with sodium arsenite at 125 μM for 2 h to form SGs (stressed, lower row) *versus* untreated cells (upper row). **(E)** HeLa cells exposed to sodium arsenite at 50 μM for 1 h to form SGs (stressed, lower row) *versus* untreated cells (upper row). **(F)** MCF7MDR cells exposed to sodium arsenite at 500 μM for 1 h to form SGs (stressed, lower row) *versus* untreated cells (upper row). **(G)** Operetta analysis of the average number of SGs per cell in Vero, HEK293, MCF7, T47D, HeLa and MCF7MDR cells. Contrast and brightness in all images were adjusted uniformly across the field of view. Scale bar = 10 μM. N = 3 and * = $p < 0.05$. Data is expressed as the mean ± standard error of the mean.

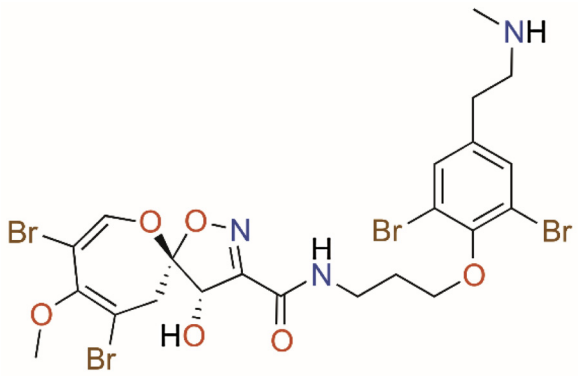

Fig. 2. The chemical structure of the marine natural product alkaloid, psammaplysin F.

MCF7MDR cells were seeded in a 24-well plate onto coverslips at a density of 150,000 cells per well and allowed to incubate overnight at 37 °C. HEK293, MCF7 and T47D cells were then stressed in media containing 125 μM of SA (Sigma) for 2 h, Vero and MCF7MDR cells were stressed in media containing 500 μM of SA for 1 h and HeLa cells were stressed in media containing 50 μM of SA for 1 h in an incubator at 37 °C. The plates were then fixed with 4% PFA (Scharlau) for 30 min. at room temperature.

2.4. Inhibition of stress granule assay

Cells were trypsinised and seeded as described in the *in vitro* stress granule assay. After overnight incubation, 30 μM of psammaplysin F (resuspended in DMSO) or DMSO (vehicle control) was added for 4 h. The final concentration of DMSO in the tissue culture media was 1%. After 4 h HEK293, MCF7 and T47D cells were stressed for 2 h in media containing 125 μM of SA. Vero and MCF7MDR cells were stressed for 1 h in media containing 500 μM of SA and HeLa cells were stressed for 1 h in media containing 50 μM of SA. Cells were then fixed in 4% PFA for 30 min. at room temperature. Antibody staining was performed as described below.

2.5. Double staining (G3BP1 + TIA1)

Cells were trypsinised and resuspended as described in the *in vitro* stress granule assay. After treatment with psammaplysin F and stressing with SA the cells were fixed with 4% PFA at room temperature. After fixing the coverslips were washed with PBS (Life Technologies) and permeabilised with 1% Triton X-100 (Sigma) at room temperature for 15 min. and washed three times with PBS. The cells were incubated with 2% BSA (Sigma) at room temperature for 1 h, the BSA was removed and the cells were incubated with anti-G3BP1 antibody (Abcam, ab556574, lot: GR301189-1) for 1 h at room temperature. Subsequently, the cells were washed three times with PBS and then incubated with secondary Alexa Fluor 488 antibody (Life Technologies, A1101, lot: 1531668) for 1 h at room temperature. Cells were washed twice with PBS and then 2% BSA was added into each well for 1 h at room temperature. The BSA was removed and the cells were incubated with anti-TIA1 antibody (Abcam, ab40693, lot: GR311160-1) for 1 h. Subsequently, the cells were washed with PBS and incubated with secondary Alexa Fluor 594 antibody (Abcam, ab150076, lot: GR274252-1) for 1 h. Cells were washed twice with PBS and incubated with DAPI (Life Technologies) for 5 min. Following this, cells were washed with PBS and the coverslips were mounted onto microscope slides and left to dry overnight at room temperature and protected from light. Cells were later visualised using the Olympus FV10-ASW 4.2 confocal image acquisition software. Incubation with secondary antibodies alone did not give any detectable background signal.

2.6. Western blot

Cells were seeded and treated as described in the inhibition of stress granule assay. After treatment, cells were treated with trypsin and pelleted in a centrifuge for 5 min. at 0.3 rcf. The cells were resuspended in 1 mL of ice cold PBS and re-spun for 5 min. at 0.3rcf. PBS was removed and the cell pellet was resuspended in 1X protease inhibitor (Thermoscientific) in RIPA buffer (Sigma) for 20 min. with agitation occurring every 5 min. After 20 min. the cell lysates were spun for 20 min. at 4 °C at max speed. The supernatant was removed and loading buffer was added and the samples denatured for 5 min. at 95 °C. Equal amounts of total protein were run on SDS-PAGE, transferred to PVDF membrane (Immobilon-P) by wet transfer at 4 °C at 100 V for 1.5 h. The membranes were blocked for 1 h at room temperature in 5% BSA or 5% milk powder in TBST. Membranes were incubated with primary antibodies (β actin - GeneTex, GXT100313, lot: 42305, α tubulin - Abcam, ab18251, lot: CR245493-1, phosphorylated eIF2α - Cell Signalling Technology 9721S, lot: 15, eIF2α – Life Technologies AH00802, lot: QF215110 and HRI – Santa Cruz Biotechnology lot: E0217) overnight and HRP-conjugated secondary antibodies (mouse HRP- Invitrogen and rabbit HRP-Li-Cor) for 1 h at room temperature. Membranes underwent ECL detection on a Bio-Rad or Odyssey imager.

2.7. In vitro combination assay

Cells were trypsinised and resuspended as described in the *in vitro* stress granule assay. 300 cells for MCF7 and 400 cells for HeLa and MCF7MDR cells were seeded per well in a 384-well plate and incubated overnight in an incubator at 37 °C. Psammaplsyin F (2, 3, 4, 5, 6, 7, 8, 9 and 10 μM), bortezomib (1, 2, 3, 4, 5, 6, 7, 8 and 9 nM) or sorafenib (2, 3, 4, 5, 6, 7, 8, 9 and 10 μM) were added in combination into each well and incubated for 68 h at 37 °C. After 68 h 5 μL of AlamarBlue was added into each well, incubated for 4 h and then the fluorescence was read using the EnVision 2105 plate reader.

2.8. In vitro combination analysis

Combination data was analysed using the Chou-Talalay method based on the median effect equation (Chou and Talalay, 1984). Combination index values were obtained using the Compusyn 1.0 software.

2.9. Operetta assay and analysis

Cells were plated in Perkin Elmer 96 well plates and processed for the inhibition of stress granule assay as described above. 25,000 cells were plated for HEK293, MCF7, T47D and Vero cells, 15,000 for HeLa cells, 10,000 cells for MCF7MDR cells and incubated overnight at 37 °C. The cells were treated as described in the inhibition of stress granule assay and were stained for G3BP1 and TIA1 to visualise SG and DAPI to visualise nuclei. Harmony high-content analysis software was used to analyse 25 random fields of view for each parameter in triplicate, totalling 225 fields of view for n = 3. The number of SGs were analysed by recognising any intensity over 0.060 for Vero, HEK293, MCF7, T47D and MCF7MDR cells and 0.1 for HeLa cells. The average number of SGs was determined by dividing the number of SGs by the number of nuclei in each parameter.

2.10. Densitometry analysis of western blot

β actin (GeneTex, GXT100313, lot: 42305) or α tubulin (Abcam, ab18251, lot: CR245493-1) were used as loading controls and to normalise the data. The signals for phosphorylated eIF2α (Cell Signalling Technology 9721S, lot: 15) were divided by those of the loading controls. These values were normalised with the highest signal intensity being equivalent to 1 to achieve the ratio of phosphorylated eIF2α to the loading control.

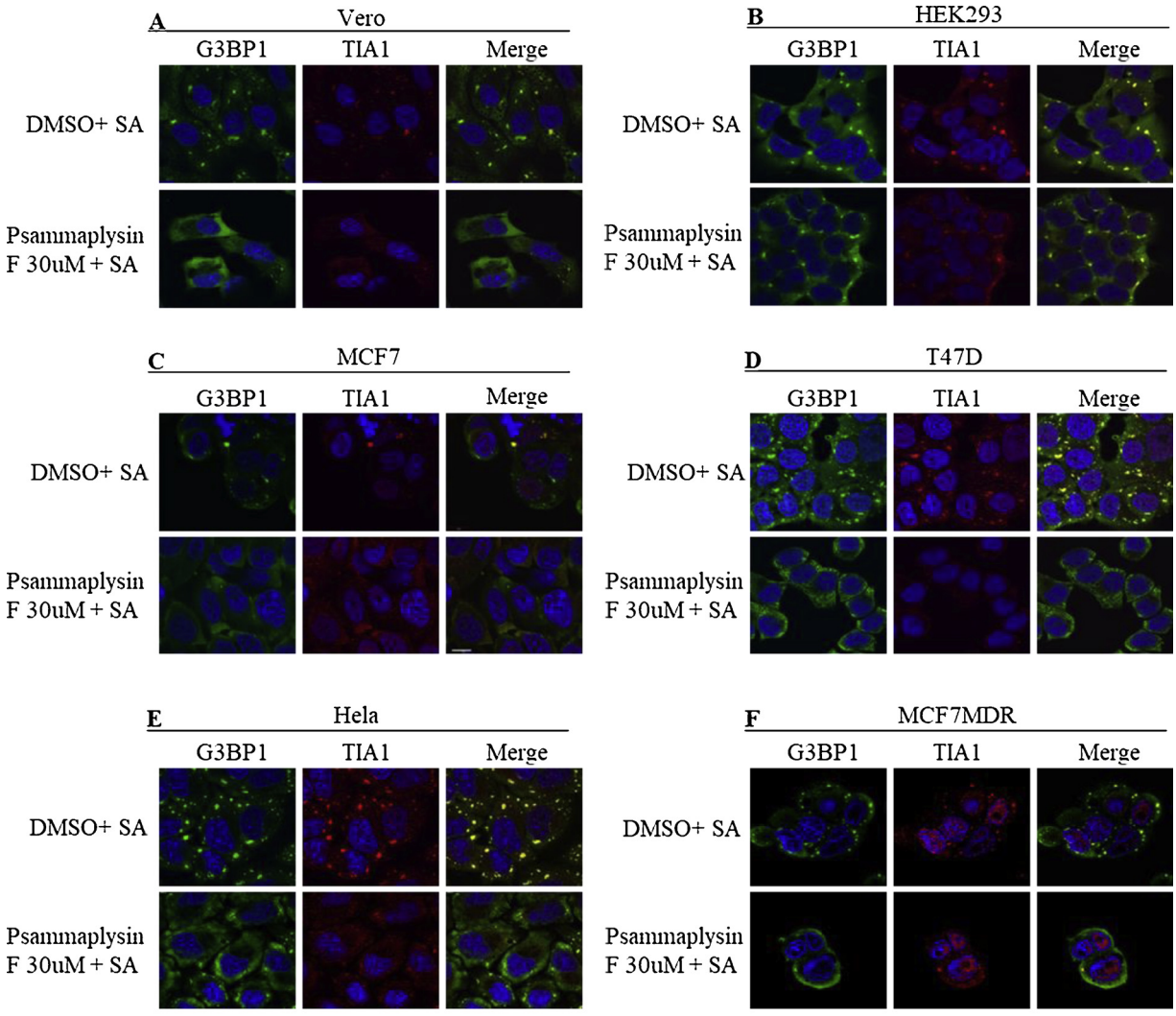

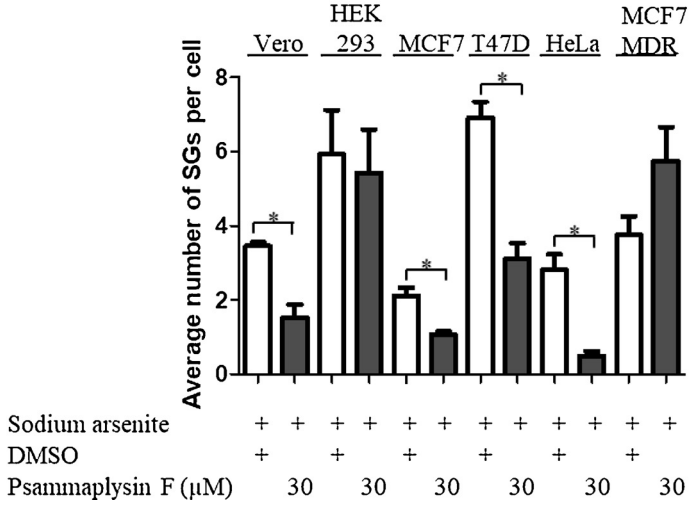

Fig. 3. Psammaplysin F reduces stress granule formation in Vero, MCF7, T47D and HeLa cells. (A) Vero cells were treated with DMSO (Vehicle control) or psammaplysin F for 4 h and then stressed with SA for 1 h at 500 μM, fixed and visualised for G3BP1, TIA1 and nuclear staining. **(B)** HEK293, **(C)** MCF7 and **(D)** T47D cells were treated with DMSO (vehicle control) or psammaplysin F for 4 h and then stressed with SA for 2 h at 125 μM fixed and visualised for G3BP1, TIA1 and nuclear staining. **(E)** HeLa cells were treated with DMSO (vehicle control) or psammaplysin F for 4 h and then stressed with SA for 1 h at 50 μM fixed and visualised for G3BP1, TIA1 and nuclear staining. **(F)** MCF7MDR cells were treated with DMSO (vehicle control) or psammaplysin F for 4 h and then stressed with SA for 1 h at 500 μM fixed and visualised for G3BP1, TIA1 and nuclear staining. **(G)**Operetta analysis of SGs in Vero, HEK293, MCF7, T47D and HeLa cells. Contrast and brightness in all images were adjusted uniformly across the field of view. Scale bar = 10 μM. N = 3 and *=$p < 0.05$. Data is expressed as the mean ± standard error of the mean.

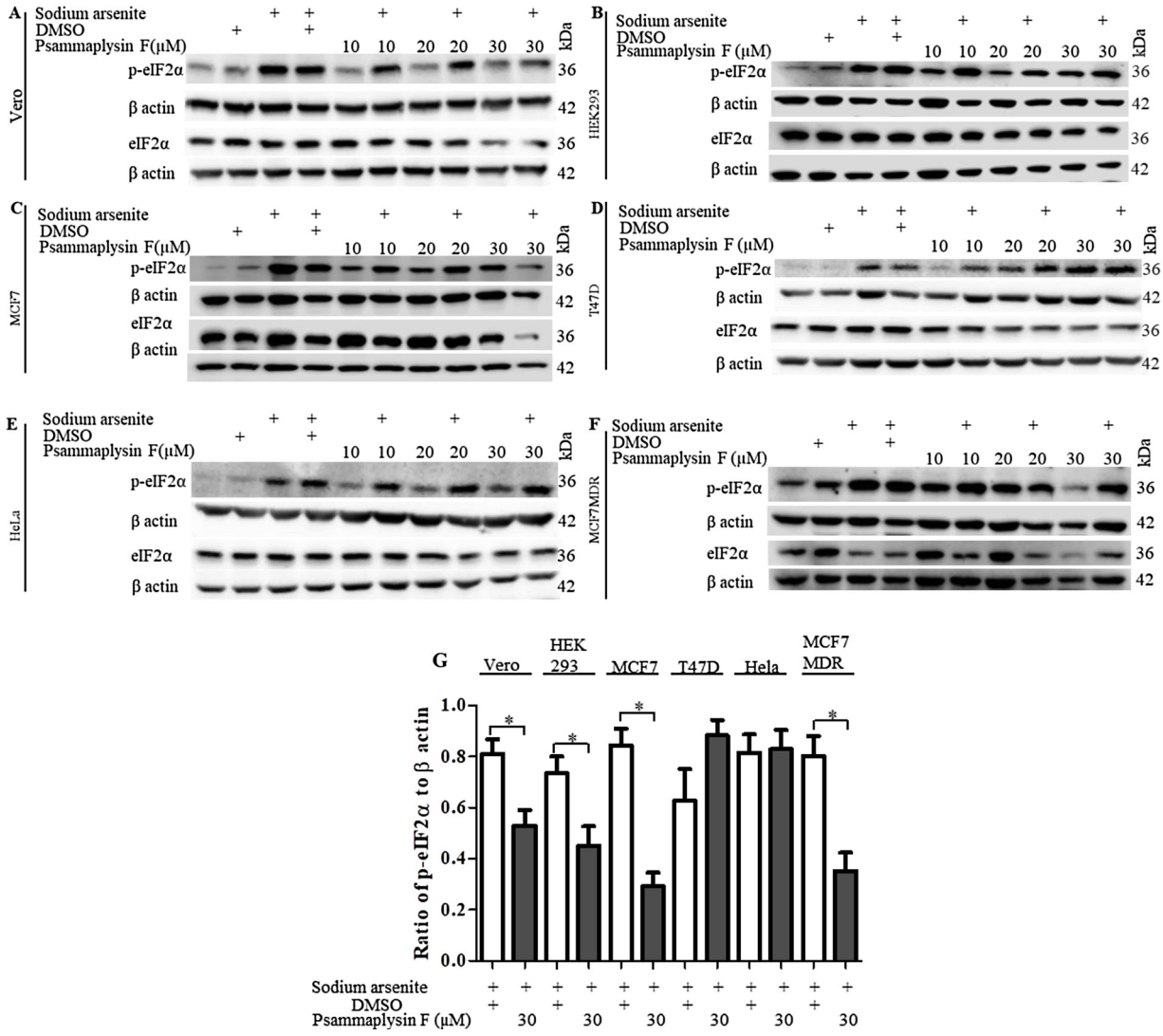

Fig. 4. Psammaplysin F reduces the phosphorylation of eIF2α in Vero, HEK293, MCF7 and MCF7MDR cells. (A) Vero cells were treated with increasing concentrations of psammaplysin F (10–30 μM) and stressed with sodium arsenite for 1 h at 500 μM. Protein was extracted and visualised for phosphorylated eIF2α (p-eIF2α), eIF2α and β actin. **(B)** HEK293, **(C)** MCF7 and **(D)** T47D cells were treated with increasing concentrations of psammaplysin F (10–30 μM) and stressed with sodium arsenite for 2 h at 125 μM. Protein was extracted and visualised for phosphorylated eIF2α (p-eIF2α), eIF2α and β actin. **(E)** HeLa cells were treated with increasing concentrations of psammaplysin F (10–30 μM) and stressed with sodium arsenite for 1 h at 50 μM. Protein was extracted and visualised for phosphorylated eIF2α (p-eIF2α), eIF2α and β actin. **(F)** MCF7MDR cells were treated with increasing concentrations of psammaplysin F (10–30 μM) and stressed with sodium arsenite for 1 h at 500 μM. Protein was extracted and visualised for phosphorylated eIF2α (p-eIF2α), eIF2α and β actin. **(G)** Analysis of the ratio of phosphorylated eIF2α to β actin for all cell lines. N = 3. *= $p < 0.05$. Data is expressed as mean ± standard error of the mean.

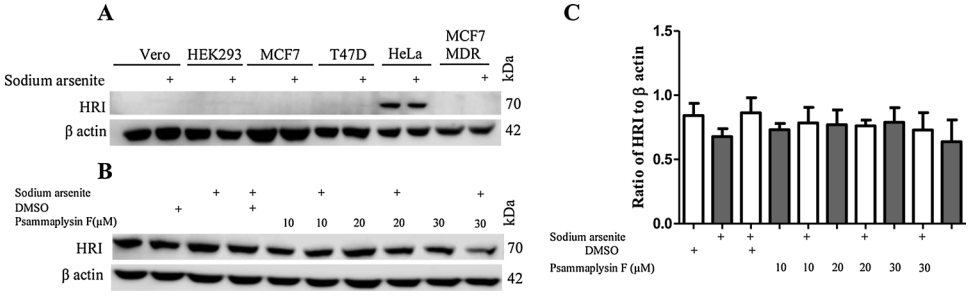

Fig. 5. HRI is overexpressed in HeLa cells and is not influenced by psammaplysin F. (A) HRI protein analysis, by Western blot, is shown for untreated and SA-treated cells for each cell line. HEK293, MCF7 and T47D cells were stressed with SA for 2 h at 125 μM. Vero cells were stressed with SA for 1 h at 500 μM, HeLa cells were stressed with SA for 1 h at 50 μM and MCF7MDR cells were stressed for 1 h at 500 μM. Protein was extracted and visualised for HRI and β actin. **(B)** HeLa cells were treated with increasing concentrations of psammaplysin F (10-30 μM) and stressed with sodium arsenite for 1 h at 50 μM. Protein was extracted and visualised for HRI and β actin. **(C)** Analysis of the ratio of HRI to β actin in HeLa cells. N = 3. Data is expressed as the mean ± standard error of the mean.

2.11. Statistical analysis

Results were expressed as the mean ± standard error. The significance of differences among experimental groups was assessed by students *t*-test or one-way analysis of variance (ANOVA) followed by the Tukey test to compare groups. Results were considered statistically significant when the *p* value < 0.05. All analyses were performed by Graph Pad prism 5 software, with the exception of the average number

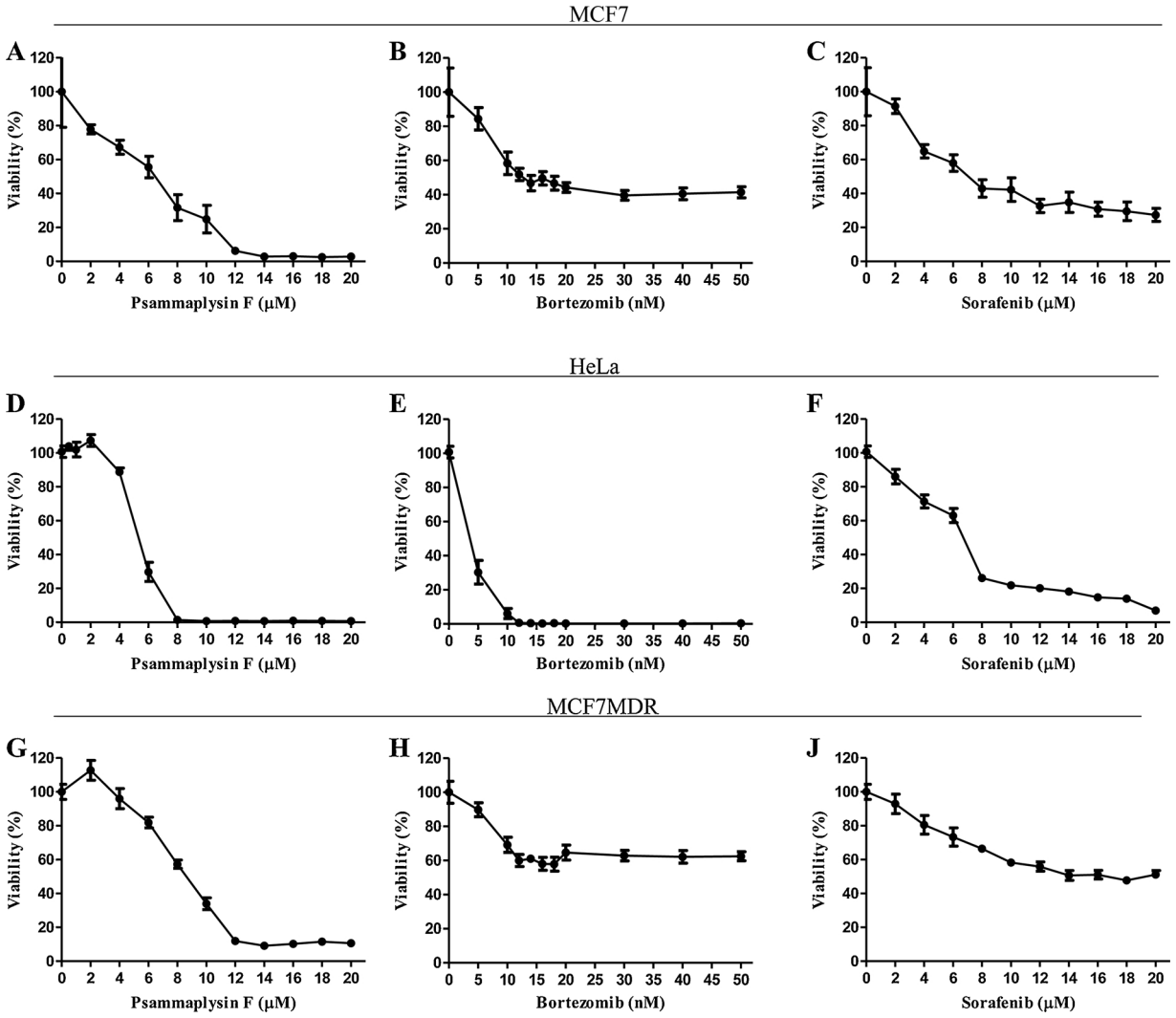

Fig. 6. Dose response curves of psammaplysin F, bortezomib and sorafenib in MCF7, HeLa and MCF7MDR cells. MCF7 cells were treated with 9 concentrations of (A) psammaplysin F (2–20 μM), (B) bortezomib (5–50 nM) and (C) sorafenib (2–20 μM). The curves were generated by plotting the mean viability against the concentration of psammaplysin F, bortezomib or sorafenib. HeLa cells were treated with 9 concentrations of (D) psammaplysin F (2–20 μM), (E) bortezomib (5–50 nM) and (F) sorafenib (2–20 μM). The curves were generated by plotting the mean viability against the concentration of psammaplysin F, bortezomib or sorafenib. MCF7MDR cells were treated with 9 concentrations of (G) psammaplysin F (2–20 μM), (H) bortezomib (5–50 nM) and (I) sorafenib (2–20 μM). The curves were generated by plotting the mean viability against the concentration of psammaplysin F, bortezomib or sorafenib. N = 3. Data is expressed as the mean ± error of the mean.

Table 1
Ic_{50} values in all cell lines.

	IC_{50}		
Cell lines	Psammaplysin F (μM)	Bortezomib (nM)	Sorafenib (μM)
Vero	5.2	8.1	7.6
HEK293	4.7	3.8	4.8
MCF7	7.6	13.2[a]	7.1
T47D	8.6	11.4	6.5
HeLa	5.2	9.2	6.7
MCF7MDR	7.8	9.1[b]	17.2[a]

Note:
[a] Concentration that caused max cell death (40%).
[b] Concentration that caused max cell death (30%).

of SGs per cell and the combination index, which was performed using the Intuitive Harmony® High Content Imaging and Analysis Software and Compusyn software.

3. Results

A screening campaign was designed using 132 natural products to identify compounds that could disrupt SG formation in an *in vitro* assay using tissue-cultured cells. The compounds were obtained from the Davis Open Access Compound Library (Griffith Institute for Drug Discovery, Griffith University, Australia) which currently consists of 472 distinct compounds. The majority (53%) of which are natural products that have been obtained from Australian natural sources, such as endophytic fungi (Davis, 2005), plants (Levrier et al., 2013), macrofungi (Choomuenwai et al., 2012), and marine invertebrates (Barnes et al., 2010). Approximately 28% of this library contains semi-synthetic natural product analogues (Barnes et al., 2016), while a smaller percentage (19%) are known commercial drugs or synthetic compounds inspired by natural products. Psammaplysin F was identified following the preliminary screen of the 132 compounds as it displayed promising activity which blocked SG formation. The preliminary data from the original screen was validated as described below.

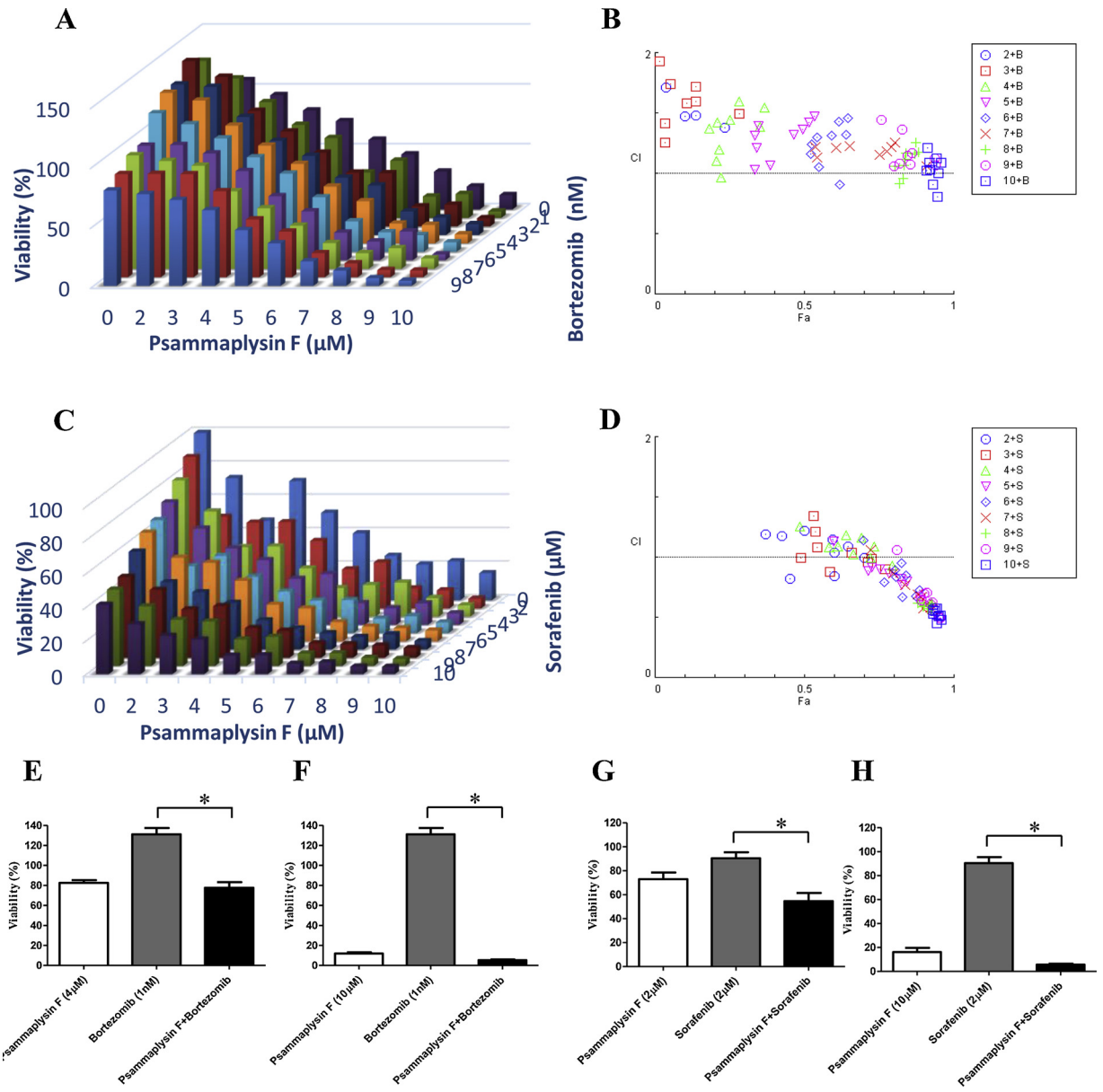

Fig. 7. Effect of psammaplysin F and two chemotherapeutics drugs; sorafenib and bortezomib in MCF7 cells. (A) MCF7 cells were treated with the indicated concentrations of psammaplysin F and sorafenib and assessed for cell viability by alamarBlue assay. (B) Combination index (CI) for psammaplysin F and sorafenib in MCF7 cells was calculated using CompuSyn software. (C) MCF7 cells were treated with the indicated concentrations of psammaplysin F and bortezomib and assessed for cell viability by alamarBlue assay. (D) Combination index (CI) for psammaplysin F and bortezomib in MCF7 cells. (E) MCF7 cells were treated with psammaplysin F at 4 μM, bortezomib at 1 nM and psammaplysin F and bortezomib combined at 72 h. (F) MCF7 cells were treated with psammaplysin F at 10 μM, bortezomib at 1 nM and psammaplysin F and bortezomib combined at 72 h. (G) MCF7 cells were treated with psammaplysin F at 2 μM, sorafenib at 2 μM and psammaplysin F and bortezomib combined at 72 h. (H) MCF7 cells were treated with psammaplysin F at 10 μM, sorafenib at 2 μM and psammaplysin F and bortezomib combined at 72 h. CI < 1, = 1, and > 1 stand for synergistic, additive, and antagonistic effects, respectively. "Fa" refers to inhibitory rate. Within the internal legend key for panels B and D the nomenclature is sequential; 2 + B = 2μM psammaplysin F + bortezomib (1–9 nM), 3 + B = 3 μM psammaplysin F + bortezomib (1–9 nM). Data is expressed as mean ± standard error of the mean. N = 3.

3.1. Sodium arsenite causes stress granule formation

A study by Fournier et al., in 2010 (Fournier et al., 2010) found that inhibiting the formation of SGs in HeLa cells by knocking down HRI, increased the cytotoxicity of a chemotherapeutic, bortezomib. The aim of this research was to identify a natural product-derived compound that inhibited the formation of SGs and this would be used to validate the hypothesis that compounds with this mechanism of action could be used in a potential adjuvant therapy, for use in combination with existing chemotherapeutics to reduce drug resistance in cancer cells.

To identify potential compounds, an *in vitro* stress granule assay was developed for the purposes of screening compounds that could block the process. Six cell lines, HEK293, MCF7, T47D, Vero, HeLa cells and MCF7MDR cells were evaluated to determine the optimal conditions for the formation of SGs as a result of SA treatment. SA treatment was used as it is a strong inducer of oxidative stress and results in the formation of SGs (Kedersha et al., 1999). The 6 cell lines were treated with SA concentrations ranging from (50 μM to 1 mM) at time points ranging from 30 min. to 2 h. After SA treatment, cells were stained with antibodies against G3BP1 and TIA1 and visualised using the Olympus FV10-ASW 4.2 confocal image acquisition software. All 6 cell lines could form SGs after treatment with SA (Fig. 1A–F). The optimum time

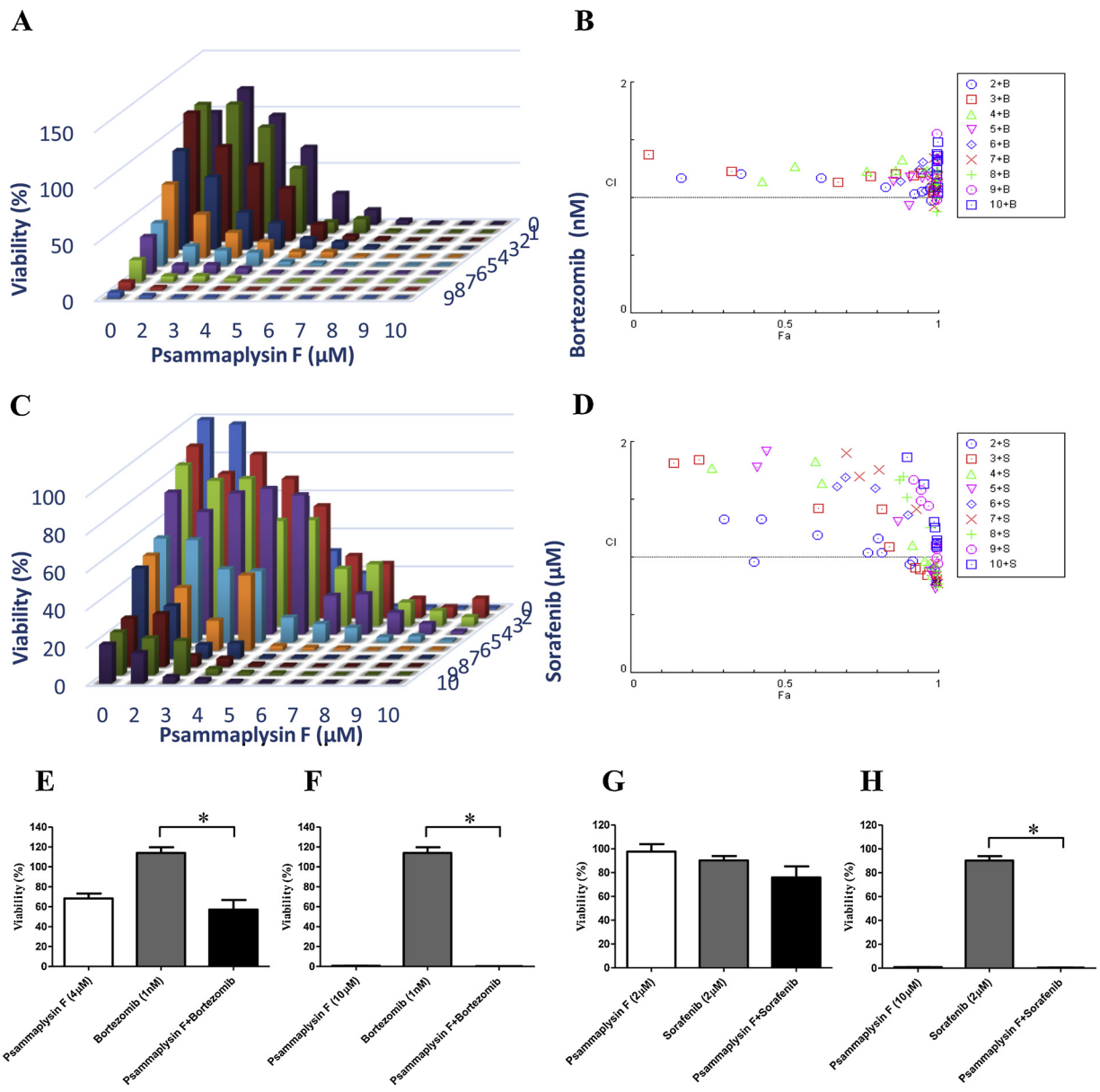

Fig. 8. Effect of psammaplysin F and two chemotherapeutics drugs; sorafenib and bortezomib in HeLa cells. (A) HeLa cells were treated with the indicated concentrations of psammaplysin F and sorafenib and assessed for cell viability by alamarBlue assay. (B) Combination index (CI) for psammaplysin F and sorafenib in HeLa cells was calculated using CompuSyn software. (C) HeLa cells were treated with the indicated concentrations of psammaplysin F and bortezomib and assessed for cell viability by alamarBlue assay. (D) Combination index (CI) for psammaplysin F and bortezomib in HeLa cells. (E) HeLa cells were treated with psammaplysin F at 4 μM, bortezomib at 1 nM and psammaplysin F and bortezomib combined at 72 h. (F) HeLa cells were treated with psammaplysin F at 10 μM, bortezomib at 1 nM and psammaplysin F and bortezomib combined at 72 h. (G) HeLa cells were treated with psammaplysin F at 2 μM, sorafenib at 2 μM and psammaplysin F and bortezomib combined at 72 h. (H) HeLa cells were treated with psammaplysin F at 10 μM, sorafenib at 2 μM and psammaplysin F and bortezomib combined at 72 h. CI < 1, = 1, and > 1 stand for synergistic, additive, and antagonistic effects, respectively. "Fa" refers to inhibitory rate. Within the internal legend key for panels B and D the nomenclature is sequential; 2 + B = 2 μM psammaplysin F + bortezomib (1–9 nM), 3 + B = 3 μM psammaplysin F + bortezomib (1–9 nM). Data is expressed as mean ± standard error of the mean. N = 3.

and concentration of SA was found to be 125 μM for 2 h in HEK293, MCF7 and T47D cells, 500 μM for 1 h in Vero and MCF7MDR cells and 50 μM for 1 h in HeLa cells (data not shown).

3.2. Psammaplysin F treatment results in the reduction of stress granule formation

A screen to discover compounds that can impair SG formation was performed to identify candidate compounds for further biological evaluation. The assay was performed by pre-treating cells with each candidate compound for 4 h at 50 μM. Subsequently, all cell lines were stressed as described using the *in vitro* stress granule assay developed for this screening. However, it was found that treatment with psammaplysin F (Fig. 2) resulted in cell death, therefore, a titration from 10 to 30 μM of psammaplysin F was used. The results showed that pre-treatment with 30 μM psammaplysin F for 4 h showed promising results for SG inhibition and this concentration and time point was used for the subsequent experiments. All cell lines were treated with psammaplysin F for 4 h at 30 μM and then subsequently stressed with the optimum concentrations of SA to form SGs. These cells were then stained with antibodies against the SG markers G3BP1 and TIA1 and visualised using the confocal microscope (Fig. 3A–F) to determine if psammaplysin F could reduce the amount of SGs being formed. A visual change was observed in the SGs in Vero, MCF7, T47D, HeLa and MCF7MDR cell

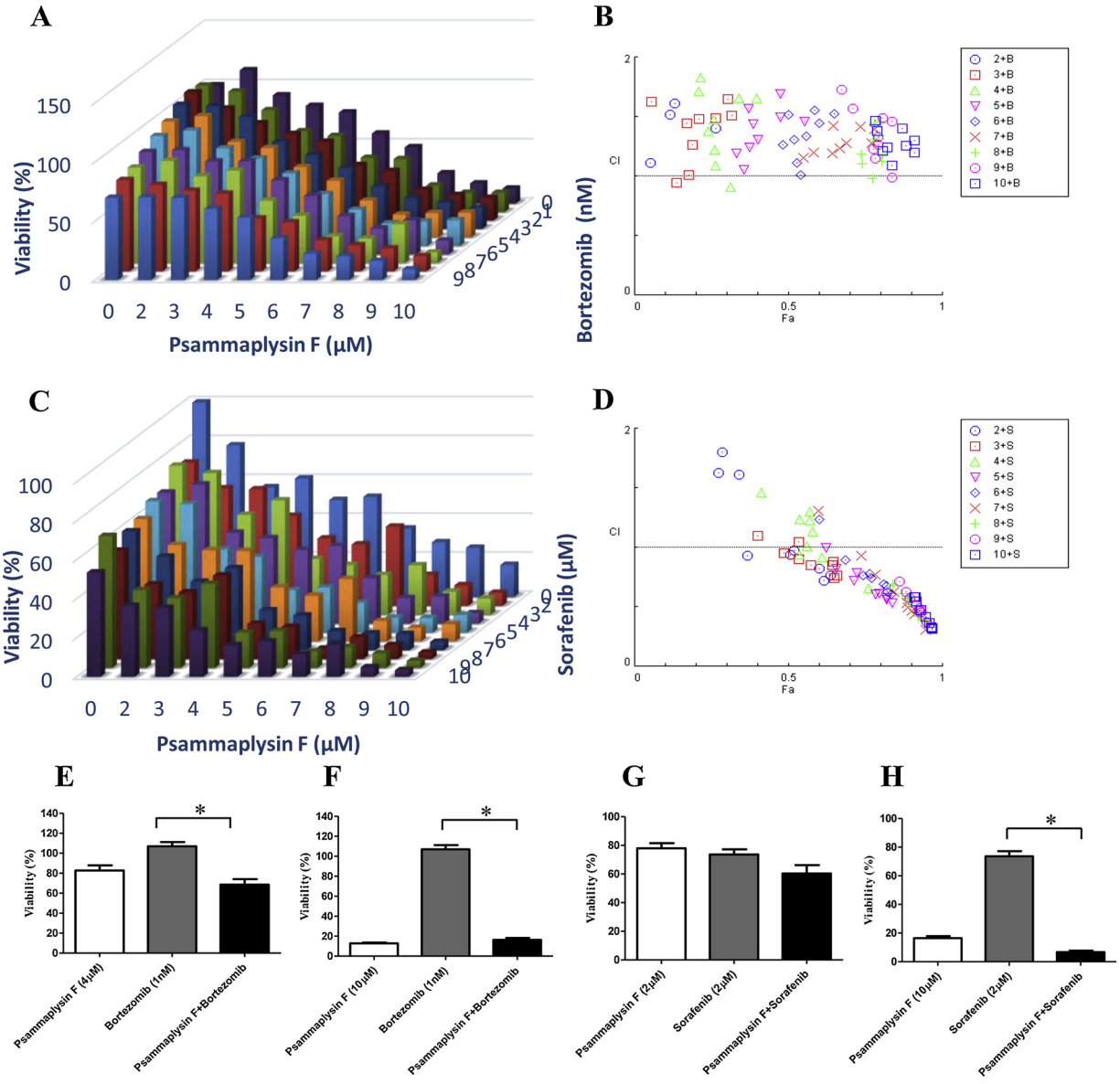

Fig. 9. Effect of psammaplysin F and two chemotherapeutics; sorafenib and bortezomib in MCF7MDR cells. (A) MCF7MDR cells were treated with the indicated concentrations of psammaplysin F and sorafenib and assessed for cell viability by alamarBlue assay. (B) Combination index (CI) for psammaplysin F and sorafenib in MCF7MDR cells was calculated using CompuSyn software. (C) MCF7MDR cells were treated with the indicated concentrations of psammaplysin F and bortezomib and assessed for cell viability by alamarBlue assay. (D) Combination index (CI) for psammaplysin F and bortezomib in MCF7MDR cells. (E) MCF7MDR cells were treated with psammaplysin F at 4 μM, bortezomib at 1 nM and psammaplysin F and bortezomib combined at 72 h. (F) MCF7MDR cells were treated with psammaplysin F at 10 μM, bortezomib at 1 nM and psammaplysin F and bortezomib combined at 72 h. (G) MCF7MDR cells were treated with psammaplysin F at 2 μM, sorafenib at 2 μM and psammaplysin F and bortezomib combined at 72 h. (H) MCF7MDR cells were treated with psammaplysin F at 10 μM, sorafenib at 2 μM and psammaplysin F and bortezomib combined at 72 h. CI $<$ 1, $=$ 1, and $>$ 1 stand for synergistic, additive, and antagonistic effects, respectively. Within the internal legend key for panels B and D the nomenclature is sequential; 2 + B = 2 μM psammaplysin F + bortezomib (1–9 nM), 3 + B = 3 μM psammaplysin F + bortezomib (1–9 nM). Data is expressed as mean ± standard error of the mean. N = 3.

lines. (Fig. 3A, C–F) Therefore, the experiments were repeated in the 96-well format and results were analysed using Harmony high-content analysis software to determine the average number of SGs per cell. It was shown that psammaplysin F significantly reduced the amount of SGs in four cell lines, Vero, MCF7, T47D and HeLa cells when compared to the control cells which were treated with the vehicle (DMSO) only and subsequently stressed with SA (Fig. 3F).

3.3. Psammaplysin F decreases the phosphorylation of eIF2a under stress

A well-documented molecular pathway resulting in the assembly of SGs is *via* the phosphorylation of eIF2a. Therefore, phosphorylation of eIF2α was assessed to determine if this was a mechanism of action for psammaplysin F. To assess this, cells were pre-treated with psammaplysin F for 4 h at 30 μM and subsequently stressed with SA as described above and total proteins were extracted from the cells. Western blot analysis was performed to determine the levels of phosphorylated eIF2α (p-eIF2α) and total eIF2α expression after treatment with psammaplysin F. The analysis of data was expressed as the ratio of p-eIF2α to β-actin and revealed a significant decrease in the ratio of p-eIF2α to β-actin in HEK293, Vero, MCF7 and MCF7MDR cell lines (Fig. 4A–C, F and G) but did not show a decrease in T47D and HeLa cells (Fig. 4D, E and G). The data did not show any significant decreases in the amount of total eIF2α in all 6 cell lines after treatment with psammaplysin F

Table 2
The combination index (CI) of psammaplysin F and bortezomib treatment on MCF7 cells.

Psammaplysin F (μM)	Bortezomib (nM)								
	1	2	3	4	5	6	7	8	9
2	–	–	–	–	–	1.71357	1.47251	1.47884	1.37763
3	1.25767	1.41597	1.93417	2.10342	1.74302	1.58604	1.60073	1.72254	1.49867
4	0.97055	1.10173	1.19736	1.37019	1.42437	1.4483	1.3889	1.60103	1.55067
5	1.0327	1.06813	1.21391	1.3156	1.39272	1.32354	1.36851	1.42106	1.47522
6	0.9088	1.05502	1.16511	1.24307	1.2979	1.31622	1.32483	1.42882	1.46054
7	1.13423	1.2192	1.21278	1.22825	1.15534	1.18278	1.21931	1.25641	1.06004
8	0.91835	0.9572	1.06337	1.07104	1.12285	1.16983	1.16152	1.17861	1.2593
9	1.06143	1.08653	1.07289	1.1506	1.17249	1.44447	1.36334	1.07092	1.13001
10	0.80685	0.90857	1.02632	1.03138	1.09018	1.00583	1.217	1.12451	1.092

Table 3
The combination index (CI) of psammaplysin F and bortezomib treatment on HeLa cells.

Psammaplysin F (μM)	Bortezomib (nM)								
	1	2	3	4	5	6	7	8	9
2	–	1.17359	1.20677	1.17202	1.09228	1.03136	1.05691	0.97345	1.08163
3	1.37073	1.23025	1.13614	1.18808	1.20496	1.19395	1.21377	1.0385	1.06162
4	1.14248	1.27522	1.2288	1.23855	1.32995	1.21886	1.23715	1.08752	1.14409
5	0.93063	1.14474	1.17796	1.1687	1.18632	1.06971	1.04905	0.98336	1.04233
6	1.13995	1.06106	1.24143	1.30658	1.22961	1.09242	1.1343	1.13034	1.14466
7	0.92233	1.06108	1.15573	1.14029	1.08209	1.34422	1.0741	1.12924	1.18438
8	0.87755	0.99587	1.10979	1.12553	1.15507	1.11727	1.23136	1.22754	1.3493
9	0.97988	1.13011	1.16897	1.1985	1.26063	1.36347	1.33369	1.32585	1.55797
10	1.03819	1.09333	1.20014	1.2591	1.31807	1.37704	1.36902	1.33044	1.47929

Table 4
The combination index (CI) of psammaplysin F and bortezomib treatment on MCF7MDR cells.

Psammaplysin F (μM)	Bortezomib (nM)								
	1	2	3	4	5	6	7	8	9
2	–	1.11158	–	–	2.18828	1.52118	1.61266	1.40181	–
3	0.94573	1.01187	1.62419	1.2635	1.44775	1.48516	1.4907	1.51094	1.65038
4	0.90711	1.08998	1.22086	1.38128	1.47149	1.71461	1.82972	1.6593	1.65365
5	1.05141	1.19462	1.24503	1.30677	1.43938	1.57014	1.49781	1.46317	1.68975
6	1.0109	1.11467	1.26397	1.3083	1.33854	1.51701	1.44763	1.55715	1.52622
7	1.15311	1.1954	1.19333	1.23659	1.28157	1.42654	1.27711	1.41874	1.3941
8	0.98449	1.10717	1.18255	1.12657	1.184	1.30874	1.34442	1.44378	1.45956
9	0.9864	1.14966	1.22916	1.26302	1.32804	1.57032	1.72479	1.48749	1.46143
10	1.08932	1.21524	1.24481	1.38349	1.46531	1.25563	1.19918	1.40235	1.30311

Table 5
The combination index (CI) of psammaplysin F and sorafenib treatment on MCF7 cells.

Psammaplysin F (μM)	Sorafenib (μM)								
	2	3	4	5	6	7	8	9	10
2	0.82174	1.1888	1.18032	0.84619	1.21812	1.04154	1.14908	1.08775	0.99292
3	0.99765	0.87822	1.08626	1.21496	1.34738	1.04281	0.96067	0.98842	0.90239
4	1.25799	1.08312	1.08764	1.02522	1.18495	0.9991	1.16545	1.08704	0.93423
5	1.13059	0.88737	0.91829	0.901	0.8675	0.76875	0.82498	0.79851	0.6481
6	0.79644	0.6683	1.14343	0.8359	0.89257	0.67473	0.85223	0.94975	0.72671
7	1.06029	0.86546	0.76977	0.57959	0.69367	0.67162	0.61429	0.58624	0.56803
8	0.61666	0.58765	0.59737	0.57278	0.60481	0.5657	0.6226	0.6204	0.61547
9	0.63957	0.68033	1.05879	0.69675	0.61208	0.70361	0.62765	0.49623	0.49292
10	0.45437	0.5293	0.56329	0.5517	0.57364	0.51026	0.57737	0.48033	0.52047

when compared to the controls.

3.4. HRI is overexpressed in HeLa cells and is not influenced by psammaplysin F

HRI, as mentioned previously, is a kinase involved in phosphorylating eIF2α during oxidative stress. Therefore, the protein levels of HRI with and without stress were assessed by western blot to determine if the levels were changing in each cell line. Surprisingly, the levels of HRI were not detectable in Vero, HEK293, MCF7, T47D and MCF7MDR cell lines but were expressed at high levels in HeLa cells (Fig. 5A). Therefore the levels of HRI in HeLa cells were assessed after

Table 6
The combination index (CI) of psammaplysin F and sorafenib treatment on HeLa cells.

Psammaplysin F (μM)	Sorafenib (μM)								
	2	3	4	5	6	7	8	9	10
2	0.96253	1.33131	1.32853	1.19509	1.03925	1.03967	1.16537	0.93591	0.96899
3	1.81604	1.84535	2.02003	1.42671	1.08804	0.90871	0.89678	1.42027	0.84751
4	1.76952	2.0542	2.42375	1.64334	1.82912	1.10361	0.96884	0.93501	0.84573
5	1.77884	1.9196	2.60845	1.30488	0.88117	0.73069	0.82331	0.83663	0.78589
6	1.60945	1.6914	1.59437	1.36935	0.90962	0.77349	0.79559	0.89223	0.80854
7	1.69954	1.89953	1.76022	1.41312	0.94554	0.84658	0.79067	0.80817	0.77213
8	1.51805	1.67212	1.70162	1.25763	0.84864	0.7459	0.88363	0.77211	0.91862
9	1.48762	1.66853	1.58266	1.44438	1.11989	1.08286	1.06773	0.99408	0.94841
10	1.86247	1.63272	1.31048	1.25535	1.1265	1.14722	1.12246	1.08704	1.10454

Table 7
The combination index (CI) of psammaplysin F and sorafenib treatment on MCF7MDR cells.

Psammaplysin F (μM)	Sorafenib (μM)								
	2	3	4	5	6	7	8	9	10
2	0.93361	1.62729	1.80171	1.61303	0.93877	0.97175	0.72359	0.82398	0.76154
3	1.10047	0.94985	0.89871	0.85086	1.04926	0.74615	0.76214	0.84938	0.88251
4	0.93709	1.46377	1.009	0.91817	1.23639	1.13217	1.22913	1.30069	0.65739
5	0.82524	0.72257	0.99926	0.60432	0.78273	0.60989	0.55894	0.57589	0.53526
6	0.89404	0.76787	1.23306	0.74541	0.77789	0.62812	0.60281	0.69076	0.67966
7	1.30864	0.77389	0.92976	0.62509	0.49513	0.46618	0.30572	0.43675	0.53463
8	0.68053	0.69561	0.60887	0.42721	0.53464	0.47041	0.57412	0.56601	0.38641
9	0.57368	0.62816	0.71355	0.46958	0.45244	0.51637	0.46902	0.48645	0.3726
10	0.4758	0.54601	0.41634	0.58674	0.58313	0.36618	0.31641	0.32989	0.31943

treatment with psammaplysin F (10, 20 and 30 μM) for 4 h to determine if HRI was being reduced in the cell (Fig. 5B). It was found that there was no significant difference in protein levels of HRI between vehicle control and cells treated with psammaplysin F (Fig. 5C).

3.5. Cytotoxic effect of psammaplysin F combined with bortezomib and sorafenib in MCF7, HeLa and MCF7MDR cells

Inhibiting stress granules in HeLa cells by knockdown of HRI and treating these cells with bortezomib has previously been shown to result in an increase of efficacy to bortezomib (Fournier et al., 2010). To determine if this effect could be replicated using compounds, psammaplysin F was used to inhibit the formation of SGs in place of HRI knockdown and the cell viability was assessed. The concentrations used to determine the IC_{50}s of psammaplysin F were 2, 4, 6, 8, 10, 12, 14, 16, 18 and 20 μM, bortezomib was 5, 10, 12, 14, 16, 18, 20, 30, 40 and 50 nM and for sorafenib were 2, 4, 6, 8, 10, 12, 14, 16, 18 and 20 μM. The IC_{50} values for psammaplysin F and sorafenib in MCF7 cells are 7.6 μM and 7.1 μM respectively (Fig. 6A and C). The IC_{50} of bortezomib could not be determined for MCF7 cells as cell viability did not fall below 50% (Fig. 6B). The IC_{50} values for psammaplysin F, bortezomib and sorafenib for HeLa cells are 5.2 μM, 9.2 nM and 6.7 μM respectively (Fig. 6D, E and F) and the IC_{50} value for psammaplysin F in MCF7MDR cells was 7.8 μM (Fig. 6G). The IC_{50} values for bortezomib and sorafenib could not be calculated in MCF7MDR cells as cell viability did not fall below 50% (Fig. 6H and I). Table 1 shows the IC_{50} values for all cell lines.

The concentrations chosen for psammaplysin F, bortezomib and sorafenib for the combinational assay were determined from the IC_{50} curves. As HeLa cells were the most sensitive to all the compounds 10 μM was chosen as the maximum concentration for psammaplysin F and sorafenib and 9 nM for bortezomib. The final concentrations used for the combinational assay were 2, 3, 4, 5, 6, 7, 8, 9 and 10 μM for psammaplysin F, 1, 2, 3, 4, 5, 6, 7, 8, and 9 nM for bortezomib and 2, 3, 4, 5, 6, 7, 8, 9 and 10 μM for sorafenib. It was found that the combination of bortezomib with psammaplysin F, and sorafenib with psammaplysin F decreased the cell viability when compared to the compounds alone for all cell lines (Fig. 7A and C, Fig. 8A and C and Fig. 9A and C). A significant decrease in cell viability was observed in MCF7 cells after treatment with psammaplysin F at 4 μM and bortezomib at 1 nM when compared to bortezomib alone (Fig. 7E). A significant decrease was also observed at a higher concentration of psammaplysin F (10 μM) when combined with bortezomib at 1 nM compared to bortezomib alone (Fig. 7F). Similar decreases in cell viability were seen in MCF7 cells after treatment with sorafenib. Treatment with psammaplysin F as low as 2 μM combined with sorafenib at 2 μM showed a significant decrease in cell viability when compared to sorafenib alone (Fig. 7G). There was also a significant decrease in cell viability compared to sorafenib alone when combining psammaplysin F at 10 μM and sorafenib at 2 μM (Fig. 7H). A significant decrease in cell viability was seen in HeLa cells when combining psammaplysin F at 2 μM and 10 μM with bortezomib at 1 nM when compared to bortezomib alone (Fig. 8E and F). Interestingly in Hela cells a significant decrease in cell viability was not observed at a combination 2 μM of psammaplysin F and 2 μM of sorafenib when compared to sorafenib alone (Fig. 8G). A significant decrease was seen in cell viability when comparing sorafenib alone at 2 μM to the combination of psammaplysin F at 10 μM and sorafenib at 2 μM. MCF7MDR cells had similar decreases in cell viability as HeLa cells with significant decreases seen after treatment with psammaplysin F at 2 μM and 10 μM with bortezomib at 1 nM when compared to bortezomib alone (Fig. 9E and F). A significant decrease in cell viability was not observed after treatment with psammaplysin F at 2 μM and 2 μM of sorafenib when compared to sorafenib alone (Fig. 9G). There was a significant decrease seen in the cell viability of MCF7MDR cells after treatment with a combination of 10 μM of psammaplysin F and 2 μM of sorafenib when compared to sorafenib alone (Fig. 9H).

As a result of a significant decrease in cell viability in all cell lines after treatment with psammaplysin F and bortezomib or sorafenib, the effects were analysed using the Chou-Talalay method to determine the combination index (CI) values. This method is used to determine if the effect of the combined compounds are synergistic, additive or

antagonistic where CI < 1, CI = 1 or CI > 1 respectively. A slight synergism was observed in all cell lines after treatment with psammaplysin F and bortezomib. The highest synergistic value for MCF7 was 0.80685 at a combination of psammaplysin F at 10 μM and bortezomib at 1 nM (Table 2), HeLa was 0.87755 at a combination of psammaplysin F at 8 μM and bortezomib at 1 nM (Table 3) and MCF7MDR was 0.90711 at a combination of psammaplysin F at 4 μM and bortezomib at 1 nM (Table 4). In contrast to this, combining psammaplysin F with sorafenib resulted in strong synergism in MCF7 and MCF7MDR cell lines and medium synergism in HeLa cells. The highest synergistic combination in MCF7 cells was at a combination of psammaplysin F at 10 μM and sorafenib at 2 μM with a CI value of 0.45437 (Table 5), in HeLa cells a combination of psammaplysin F at 5 μM and sorafenib at 6 μM gave a CI value of 0.73069 (Table 6) and MCF7MDR cells the most significant synergy was observed at a combination of psammaplysin F at 10 μM and sorafenib at 8 μM gave a CI value of 0.31641 (Table 7).

4. Discussion and conclusion

Characterisation of the biological functions of SGs has attracted significant interest in the field of cancer research because chemotherapeutics have been shown to induce the formation of SGs (Fournier et al., 2010, Kaehler 2014) and there are implications that SGs may contribute to the development of drug resistance. Therefore, a potential novel approach to the treatment of cancer is through the inhibition of SGs to increase the efficacy of chemotherapeutics. This concept was validated by the knock-out of HRI which can regulate SG formation and showed increased efficacy of the drug Bortezomib in HeLa cells (Fournier et al., 2010). To further validate this approach, it is important to identify mechanisms of compounds that may inhibit the formation of SGs and that can be applied, in conjunction with chemotherapeutic regimens, to aid in the treatment of cancer. Therefore, using compounds, especially those which may be druggable, to inhibit SGs represents a promising new direction in therapeutic approaches.

In this study we identified that the marine natural product alkaloid, psammaplysin F significantly decreased the formation of SGs in Vero, MCF7, T47D and HeLa cells in the presence of stress. Psammaplysin F had not previously been used to explore its role in SG formation, therefore, the mechanism of action had not been previously reported. The data presented here demonstrated that psammaplysin F appeared to inhibit SG formation by blocking phosphorylation of eIF2α during SA induced stress. Psammaplysin F was found to cause a significant decrease in the phosphorylation of eIF2α in Vero, HEK293, MCF7 and MCF7MDR cells when compared to the controls. Surprisingly, a decrease in the phosphorylation of eIF2α was observed in MCF7MDR cells despite no significant decrease in the amount of SGs after treatment with psammaplysin F. There was also no decrease in the phosphorylation of eIF2α in T47D or HeLa cells despite the observed decrease in the average number of SGs. To examine this, the levels of HRI expression were evaluated and the data showed that HRI levels are highest in HeLa cells and these expression levels may be able to overcome the negative regulation of eIF2α by psammaplysin F. The analysis of HRI levels in T47D cells were similar to those expressed in Vero and MCF7 cells and did not approach the expression levels seen in HeLa cells. Therefore, it is possible that psammaplysin F has a mechanism of action in these cells that regulates SG formation utilising a pathway other than *via* the phosphorylation of eIF2α. This will need to be addressed in further studies.

As mentioned previously HRI is one kinase that can phosphorylate eIF2α and is involved in the formation of SGs under SA stress. Therefore, the decrease in phosphorylation of eIF2α but not total eIF2α indicates that psammaplysin F may be affecting the ability of HRI to phosphorylate eIF2α. It was found that psammaplysin F did not influence the protein levels of HRI in HeLa cells which suggests that psammaplysin F may be influencing the phosphorylation of eIF2α through a HRI independent pathway. This would be in accord with the data seen in HeLa cells which demonstrated that when HRI expression levels are high in a cell, the activity of psammaplysin F is unable to abrogate its effect on the phosphorylation of eIF2α. Characterising the pathway or pathways that psammaplysin F acts on will need to be addressed in further studies.

Inhibiting SGs in HeLa cells by HRI knock down and treating those cells with bortezomib resulted in the increase in efficacy of bortezomib. Therefore, psammaplysin F was used to inhibit the formation of SGs in MCF7, HeLa and MCF7MDR cells and subsequently treated with bortezomib or sorafenib. An increase in efficacy of bortezomib and sorafenib was observed when combined with psammaplysin F, which suggests that psammaplysin F is responsible for the increase in efficacy. To determine if the effects of psammaplysin F and bortezomib or sorafenib were synergistic, additive or antagonistic the data was analysed using the Chou-Talalay method (Chou and Talalay, 1984). It was determined that psammaplysin F and bortezomib displayed slight synergism in MCF7, HeLa and MCF7MDR cells, however psammaplysin F and sorafenib showed a strong synergism in MCF7 and MCF7MDR cells lines and medium synergism in HeLa cells. Interestingly, both bortezomib and sorafenib can induce the phosphorylation of eIF2α through endoplasmic reticulum stress, bortezomib through proteasome inhibition (Schewe and Aguirre-Ghiso, 2009) and sorafenib through multiple kinase inhibition (Rahmani et al., 2007). The phosphorylation of eIF2α has been shown to provide some protection from sorafenib-mediated cell death as transfection of a non-nonphosphorylatable form of eIF2α significantly increased cell death in MEF cells after treatment with sorafenib (Rahmani et al., 2007). As a result of this it is possible that psammaplysin F treatment is impairing the ability of sorafenib and bortezomib to phosphorylate eIF2α and subsequently results in a response similar to the presence of a nonphosphorylatable form of eIF2α. The difference in synergism between psammaplysin F and sorafenib and psammaplysin F and bortezomib may be a result of the multiple kinase targets of sorafenib. The mechanism of action of sorafenib has not been fully characterised (Cervello et al., 2012) and it may be possible that sorafenib is inhibiting a kinase required for SG formation. Additionally, treatment with sorafenib causes apoptosis through the inhibition of phosphorylation of the eukaryotic initiation factor 4E (eIF4E), which is regulated by its phosphorylation. eIF4E has been shown to co-localise to SGs under sodium arsenite treatment (Anderson and Kedersha, 2006; Frydryskova et al., 2016) however, its role in SGs has not been extensively studied. The molecular pathways impacted by the combination of psammaplysin F with bortezomib or sorafenib will be investigated in future studies. The increase in cell death and the synergistic effect seen after combinations of psammaplysin F and bortezomib or sorafenib indicates that psammaplysin F has the potential to be used in combination with known chemotherapeutics to restore drug efficacy.

In conclusion, SGs represent a potent cellular response to challenge by chemotherapeutics. The ability of psammaplysin F to significantly reduce the amount of phosphorylated eIF2α and subsequent SG formation in several cell lines suggests a potential lead in the development of anti-cancer drugs. Moreover, the work presented here builds on the work by Fournier et al. (Fournier et al., 2010), which demonstrated that inhibiting SG formation by knockdown of the HRI gene restored the cytotoxic activity of the drug bortezomib. The use of psammaplysin F recapitulates the inhibition of eIF2α phosphorylation and subsequent inhibition of SG formation seen by HRI knock-down. Furthermore, the data presented here demonstrates the potential for use of small molecules from nature, such as psammaplysin F, to be used in combination with current FDA approved drugs to augment, enhance or restore drug efficacy.

Conflict of interest

None.

Funding

This research was funded by Griffith University. The authors acknowledge the Australian Research Council (ARC) for support towards NMR and MS equipment (Grant LE0668477 and LE0237908) and financial support (Grant LP120200339 to R.A.D.). R.A.D. holds a New Concept Grant funded by It's a Bloke Thing through the Prostate Cancer Foundation of Australia's Research Program.

Acknowledgements

R.A.D. acknowledges the NatureBank biota repository (www.griffith.edu.au/gridd) from which many of the compounds in the Davis Open Access Natural Product Library were isolated, including psammaplysin F. Compounds Australia (www.compoundsaustralia.com) is acknowledged for curating the Davis Open Access Natural Product Library, which forms part of the Open Access Compound Collection at Griffith University.

Appendix A. Supplementary data

Supplementary material related to this article can be found, in the online version, at doi:https://doi.org/10.1016/j.biocel.2019.04.008.

References

Anderson, P., Kedersha, N., 2006. RNA granules. J. Cell Biol. 172 (6), 803–808. https://doi.org/10.1083/jcb.200512082.

Anderson, P., Kedersha, N., 2009. Stress granules. Curr. Biol. 19 (10), R397–398. https://doi.org/10.1016/j.cub.2009.03.013.

Anderson, P., Kedersha, N., Ivanov, P., 2014. Stress granules, P-bodies and cancer. Biochim. Biophys. Acta. https://doi.org/10.1016/j.bbagrm.2014.11.009.

Anderson, P., Kedersha, N., Ivanov, P., 2015. Stress granules, P-bodies and cancer. Biochim. et Biophys. Acta (BBA) Gene Regul. Mech. 1849 (7), 861–870. https://doi.org/10.1016/j.bbagrm.2014.11.009.

Barnes, E.C., Said, N.A.M.B., Williams, E., Hooper, J.N.A., Davis, R.A., 2010. ChemInform abstract: ecionines A and B, two new cytotoxic pyridoacridine alkaloids from the Australian marine sponge, Ecionemia geodides. Tetrahedron 66 (1), 283–287.

Barnes, E.C., Kumar, R., Davis, R.A., 2016. The use of isolated natural products as scaffolds for the generation of chemically diverse screening libraries for drug discovery. Nat. Prod. Rep. 33 (3), 372–381. https://doi.org/10.1039/C5NP00121H.

Basmadjian, C., Zhao, Q., Bentouhami, E., Djehal, A., Nebigil, C.G., Johnson, R.A., et al., 2014. Cancer wars: natural products strike back. Front. Chem. 2, 20. https://doi.org/10.3389/fchem.2014.00020.

Bounedjah, O., Desforges, B., Wu, T.D., Pioche-Durieu, C., Marco, S., Hamon, L., et al., 2014. Free mRNA in excess upon polysome dissociation is a scaffold for protein multimerization to form stress granules. Nucleic Acids Res. 42 (13), 8678–8691. https://doi.org/10.1093/nar/gku582.

Buchan, J.R., Parker, R., 2009. Eukaryotic stress granules: the ins and out of translation. Mol. Cell 36 (6), 932. https://doi.org/10.1016/j.molcel.2009.11.020.

Cervello, M., Bachvarov, D., Lampiasi, N., Cusimano, A., Azzolina, A., McCubrey, J.A., et al., 2012. Molecular mechanisms of sorafenib action in liver cancer cells. Cell Cycle 11 (15), 2843–2855. https://doi.org/10.4161/cc.21193.

Choomuenwai, V., Andrews, K.T., Davis, R.A., 2012. Synthesis and antimalarial evaluation of a screening library based on a tetrahydroanthraquinone natural product scaffold. Bioorg. Med. Chem. 20 (24), 7167–7174. https://doi.org/10.1016/j.bmc.2012.09.052.

Chou, T.-C., Talalay, P., 1984. Quantitative analysis of dose-effect relationships: the combined effects of multiple drugs or enzyme inhibitors. Adv. Enzyme Regul. 22, 27–55. https://doi.org/10.1016/0065-2571(84)90007-4.

Cragg, G.M., Newman, D.J., 2009. Nature: a vital source of leads for anticancer drug development. Phytochem. Rev. 8 (2), 313–331. https://doi.org/10.1007/s11101-009-9123-y.

Davis, R.A., 2005. Isolation and structure elucidation of the new fungal metabolite (−)-xylariamide A a. J. Nat. Prod. 68 (5), 769–772. https://doi.org/10.1021/np050025h.

Demain, A.L., Vaishnav, P., 2011. Natural products for cancer chemotherapy. Microb. Biotechnol. 4 (6), 687–699. https://doi.org/10.1111/j.1751-7915.2010.00221.x.

Emara, M.M., Fujimura, K., Sciaranghella, D., Ivanova, V., Ivanov, P., Anderson, P., 2012. Hydrogen peroxide induces stress granule formation independent of eIF2α phosphorylation. Biochem. Biophys. Res. Commun. 423 (4), 763–769. https://doi.org/10.1016/j.bbrc.2012.06.033.

Fournier, M.J., Gareau, C., Mazroui, R., 2010. The chemotherapeutic agent bortezomib induces the formation of stress granules. Cancer Cell Int. 10, 12. https://doi.org/10.1186/1475-2867-10-12.

Frydryskova, K., Masek, T., Borcin, K., Mrvova, S., Venturi, V., Pospisek, M., 2016. Distinct recruitment of human eIF4E isoforms to processing bodies and stress granules. BMC Mol. Biol. 17 (1), 21. https://doi.org/10.1186/s12867-016-0072-x.

Ghisolfi, L., Dutt, S., McConkey, M.E., Ebert, B.L., Anderson, P., 2012. Stress granules contribute to alpha-globin homeostasis in differentiating erythroid cells. Biochem. Biophys. Res. Commun. 420 (4), 768–774. https://doi.org/10.1016/j.bbrc.2012.03.070.

Gilks, N., Kedersha, N., Ayodele, M., Shen, L., Stoecklin, G., Dember, L.M., et al., 2004. Stress granule assembly is mediated by prion-like aggregation of TIA-1. Mol. Biol. Cell 15 (12), 5383–5398. https://doi.org/10.1091/mbc.E04-08-0715.

Global Burden of Disease Cancer, C, 2017. Global, regional, and national cancer incidence, mortality, years of life lost, years lived with disability, and disability-adjusted life-years for 32 cancer groups, 1990 to 2015: a systematic analysis for the global burden of disease study. JAMA Oncol. 3 (4), 524–548. https://doi.org/10.1001/jamaoncol.2016.5688.

Hofmann, S., Cherkasova, V., Bankhead, P., Bukau, B., Stoecklin, G., 2012. Translation suppression promotes stress granule formation and cell survival in response to cold shock. Mol. Biol. Cell 23 (19), 3786–3800. https://doi.org/10.1091/mbc.E12-04-0296.

Housman, G., Byler, S., Heerboth, S., Lapinska, K., Longacre, M., Snyder, N., et al., 2014. Drug resistance in cancer: an overview. Cancers 6 (3), 1769–1792. https://doi.org/10.3390/cancers6031769.

Kaehler, C., Isensee, J., Hucho, T., Lehrach, H., Krobitsch, S., 2014. 5-Fluorouracil affects assembly of stress granules based on RNA incorporation. Nucleic Acids Res. 42 (10), 6436–6447. https://doi.org/10.1093/nar/gku264.

Kedersha, N., Anderson, P., 2007. Mammalian stress granules and processing bodies. Methods Enzymol 431, 62–81.

Kedersha, N.L., Gupta, M., Li, W., Miller, I., Anderson, P., 1999. RNA-binding proteins tia-1 and tiar link the phosphorylation of Eif-2α to the assembly of mammalian stress granules. J. Cell Biol. 147 (7), 1431–1442. https://doi.org/10.1083/jcb.147.7.1431.

Kedersha, N., Cho, M.R., Li, W., Yacono, P.W., Chen, S., Gilks, N., et al., 2000. Dynamic shuttling of tia-1 accompanies the recruitment of mRNA to mammalian stress granules. J. Cell Biol. 151 (6), 1257–1268. https://doi.org/10.1083/jcb.151.6.1257.

Kedersha, N., Stoecklin, G., Ayodele, M., Yacono, P., Lykke-Andersen, J., Fritzler, M.J., et al., 2005. Stress granules and processing bodies are dynamically linked sites of mRNP remodeling. J. Cell Biol. 169 (6), 871–884. https://doi.org/10.1083/jcb.200502088.

Levrier, C., Balastrier, M., Beattie, K.D., Carroll, A.R., Martin, F., Choomuenwai, V., et al., 2013. Pyridocoumarin, aristolactam and aporphine alkaloids from the Australian rainforest plant Goniothalamus australis. Phytochemistry 86, 121–126. https://doi.org/10.1016/j.phytochem.2012.09.019.

Liu, S., Fu, X., Schmitz, F.J., Kelly-Borges, M., 1997. Psammaplysin F, a new bromotyrosine derivative from a sponge, Aplysinella sp. J. Nat. Prod. 60 (6), 614–615. https://doi.org/10.1021/np970070s.

Lu, L., Han, A.P., Chen, J.J., 2001. Translation initiation control by heme-regulated eukaryotic initiation factor 2alpha kinase in erythroid cells under cytoplasmic stresses. Mol. Cell. Biol. 21 (23), 7971–7980. https://doi.org/10.1128/MCB.21.23.7971-7980.2001.

Matsuki, H., Takahashi, M., Higuchi, M., Makokha, G.N., Oie, M., Fujii, M., 2013. Both G3BP1 and G3BP2 contribute to stress granule formation. Genes Cells 18 (2), 135–146. https://doi.org/10.1111/gtc.12023.

McEwen, E., Kedersha, N., Song, B., Scheuner, D., Gilks, N., Han, A., et al., 2005. Heme-regulated inhibitor kinase-mediated phosphorylation of eukaryotic translation initiation factor 2 inhibits translation, induces stress granule formation, and mediates survival upon arsenite exposure. J. Biol. Chem. 280 (17), 16925–16933. https://doi.org/10.1074/jbc.M412882200.

McInerney, G.M., Kedersha, N.L., Kaufman, R.J., Anderson, P., Liljestrom, P., 2005. Importance of eIF2alpha phosphorylation and stress granule assembly in alphavirus translation regulation. Mol. Biol. Cell 16 (8), 3753–3763. https://doi.org/10.1091/mbc.E05-02-0124.

Rahmani, M., Davis, E.M., Crabtree, T.R., Habibi, J.R., Nguyen, T.K., Dent, P., et al., 2007. The kinase inhibitor sorafenib induces cell death through a process involving induction of endoplasmic reticulum stress. Mol. Cell. Biol. 27 (15), 5499–5513. https://doi.org/10.1128/mcb.01080-06.

Ramsey, D.M., Amirul Islam, M., Turnbull, L., Davis, R.A., Whitchurch, C.B., McAlpine, S.R., 2013. Psammaplysin F: a unique inhibitor of bacterial chromosomal partitioning. Bioorg. Med. Chem. Lett. 23 (17), 4862–4866. https://doi.org/10.1016/j.bmcl.2013.06.082.

Reineke, L.C., Dougherty, J.D., Pierre, P., Lloyd, R.E., 2012. Large G3BP-induced granules trigger eIF2alpha phosphorylation. Mol. Biol. Cell 23 (18), 3499–3510. https://doi.org/10.1091/mbc.E12-05-0385.

Ruiz-Ramos, R., Lopez-Carrillo, L., Rios-Perez, A.D., De Vizcaya-Ruiz, A., Cebrian, M.E., 2009. Sodium arsenite induces ROS generation, DNA oxidative damage, HO-1 and c-Myc proteins, NF-kappaB activation and cell proliferation in human breast cancer MCF-7 cells. Mutat. Res. 674 (1–2), 109–115. https://doi.org/10.1016/j.mrgentox.2008.09.021.

Schewe, D.M., Aguirre-Ghiso, J.A., 2009. Inhibition of eIF2α dephosphorylation maximizes bortezomib efficiency and eliminates quiescent multiple myeloma cells surviving proteasome inhibitor therapy. Cancer Res. 69 (4), 1545–1552. https://doi.org/10.1158/0008-5472.CAN-08-3858.

Smith, R., Rathod, R.J., Rajkumar, S., Kennedy, D., 2014. Nervous translation, do you get the message? A review of mRNPs, mRNA-protein interactions and translational control within cells of the nervous system. Cell. Mol. Life Sci. 71 (20), 3917–3937. https://doi.org/10.1007/s00018-014-1660-x.

Takahashi, M., Higuchi, M., Matsuki, H., Yoshita, M., Ohsawa, T., Oie, M., et al., 2013. Stress granules inhibit apoptosis by reducing reactive oxygen species production. Mol. Cell. Biol. 33 (4), 815–829. https://doi.org/10.1128/MCB.00763-12.

Wang, H., Naghavi, M., Allen, C., Barber, R.M., Bhutta, Z.A., Carter, A., et al., 2016. Global, regional, and national life expectancy, all-cause mortality, and cause-specific

mortality for 249 causes of death, 1980–2015: a systematic analysis for the Global Burden of Disease Study 2015. Lancet 388 (10053), 1459–1544. https://doi.org/10.1016/s0140-6736(16)31012-1.

Xu, M., Andrews, K.T., Birrell, G.W., Tran, T.L., Camp, D., Davis, R.A., et al., 2010. Psammaplysin H, a new antimalarial bromotyrosine alkaloid from a marine sponge of the genus Pseudoceratina. Bioorg. Med. Chem. Lett. 21 (2), 846–848. https://doi.org/10.1016/j.bmcl.2010.11.081.

Yagüe, E., Raguz, S., 2010. Escape from stress granule sequestration: another way to drug resistance? Biochem. Soc. Trans. 38 (6), 1537–1542. https://doi.org/10.1042/bst0381537.

Zulfiqar, B., Jones, A., Sykes, M., Shelper, T., Davis, R., Avery, V., 2017. Screening a natural product-based library against kinetoplastid parasites. Molecules 22 (10), 1715.